Strategies for Re-Use of Launch Vehicle First Stages: Uncertainty Quantification

Matthew T. Vernacchia * and Kelly J. Mathesius †
Massachusetts Institute of Technology, Cambridge, MA, 02139

This appendix describes the techniques used to quantify uncertianty in the performance and cost models used to compare first stage reuse strategies.

I. Performance-Related Uncertainties

A. Technology Uncertainties

This section describes uncertainties on the performance factors which we choose to group as the "technology choice": i.e. the specific impulse and inert mass fractions of each stage c_1, c_2, E_1, E_2.

Note this is not uncertainty about what the technology choice is - we assume that is given. Rather, given a technology choice (e.g. kerosene fuel, gas generator engine cycle, and aluminum alloy tanks), what is the remaining uncertainty in Isp and inert mass fraction?

1. Specific Impulse

The specific impulse is largely determined by the choice of propellant and engine cycle. However, there are still variations in nominal specific impulse between different engines using the same propellant and cycle and variations away from the nominal specific impulse in the operation of a given engine. These variations contribute to uncertainty in the performance of a new launch vehicle design.

We divide the sources of variation in specific impulse into two categories:

- *variation in nominal I_{sp}* - This captures variations in nominal specific impulse between different engines using the same propellant and cycle. Contributing factors (which may be uncertain at the outset of an engine development project) include chamber pressure, mixture ratio, expansion ratio, and injector c^* efficiency.
- *variation in operation* - This captures variations away from the nominal specific impulse in the operation of a given engine. Contributing factors which may vary between missions include throttling, mixture ratio control, and ambient pressure on different possible trajectories.

Uncertainty in nominal I_{sp} only exists if a new engine will be developed for the launch vehicle, or if the engine selection is yet to be made. For a particular launch vehicle, the nominal specific impulse is known once an engine is selected or developed. However, we wish our performance predictions to be representative of the population of engines using a particular technology, and thus include the variation in nominal specific impulse as an uncertainty in the model. TODO.

We model the variation in nominal I_{sp} by examining a sample of existing and historical launch vehicle engines (see Table 1; we believe that this is a comprehensive sample of all hydrogen and kerosene engines used for space launch). First, we must determine whether there are historical trends in the performance data. If there were a strong historical trend towards improving performance, then a sample of historical engines would not be representative of the performance in modern and near-future engines. However, liquid propulsion has been a mature field for some time [1], and Figure 1 shows no clear correlation between performance and year of first flight after 1975. Thus these engines are likely representative of the performance of contemporary and near-future engines.

Next, we need to quantify the uncertainty due to variation in operation. The listed specific impulse values are typically measured at design conditions; we expect that off-design operation could lower these values by 2%. For 2nd (upper) stage engines, which operate in near vacuum, this is the end of the story. For booster engines, there is also a large variation in specific impulse due the effects of altitude. Our performance model requires c_1 to be the *effective* 1st stage specific impulse, averaged over the altitudes at which an engine operates. As a crude estimate, we will assume that the effective specific impulse is the mean of the sea level and vacuum values:

*Research Assistant, Department of Aeronautics and Astronautics, 77 Massachusetts Avenue, AIAA Student Member.
†Research Assistant, Department of Aeronautics and Astronautics, 77 Massachusetts Avenue, AIAA Student Member.

Table 1 Examples of liquid propellant rocket engines used for space launch.

Engine	Use	Fuel	Cycle	I_{sp}, vacuum [s]	I_{sp}, sea level [s]	Chamber pressure [MPa]	Thrust /Weight [-]	Year of first flight
CE-20	Upper	H2	GG	443	-	6.0	35	2017
CE-7.5	Upper	H2	SC	454	-	5.8	19	2010
F-1	Booster	kero	GG	305	265	6.8	94	1967
HM7A	Upper	H2	GG	421	-	-	-	1979
HM7B	Upper	H2	GG	445	-	3.7	39	1986
J-2	Upper	H2	GG	425	-	4.9	66	1966
LE-5	Upper	H2	GG	450	-	3.6	41	1984
LE-5A	Upper	H2	Expander	452	-	4.0	44	1991
LE-5B	Upper	H2	Expander	450	348	3.6	48	2002
LE-7	Booster	H2	SC	446	339	12.7	64	1994
LE-7A	Booster	H2	SC	440	338	11.9	62	2002
Merlin 1C	Booster	kero	GG	304	266	6.8	78	2008
Merlin 1C Vacuum	Upper	kero	GG	342	-	-	-	2010
Merlin 1D	Booster	kero	GG	311	282	9.7	198	2013
Merlin 1D Vacuum	Upper	kero	GG	348	-	-	-	2013
NK-33	Booster	kero	SC	331	279	14.5	138	1969
RD-0110	Upper	kero	GG	326	-	6.8	74	1965
RD-0120	Booster	H2	SC	455	353	21.9	58	1987
RD-0124	Upper	kero	SC	359	-	15.7	52	2006
RD-107	Booster	kero	GG	313	256	5.9	86	1957
RD-107A	Booster	kero	GG	320	263	6.0	87	2001
RD-120	Upper	kero	SC	350	-	16.3	75	1985
RD-170, RD-171	Booster	kero	SC	337	309	24.5	75	1985
RD-180	Booster	kero	SC	338	311	26.7	77	2000
RD-181	Booster	kero	SC	339	312	26.3	97	2016
RD-56 (KDV-1)	Upper	H2	SC	462	-	5.6	25	2001
RL10A-3	Upper	H2	Expander	427	-	2.1	52	1963
RL10B-2	Upper	H2	Expander	465	-	4.6	49	1998
RL10C-1	Upper	H2	Expander	450	-	-	55	2014
RS-25 (SSME)	Booster	H2	SC	452	361	18.9	60	1981
RS-27A	Booster	kero	GG	302	255	4.8	93	1989
RS-68	Booster	H2	GG	410	365	10.1	50	2002
Rutherford	Booster	kero	Electric	311	-	-	70	2017
Rutherford Vacuum	Upper	kero	Electric	343	-	-	-	2017
Vulcain 1	Booster	H2	GG	431	326	10.0	85	1996
Vulcain 2	Booster	H2	GG	429	318	11.6	76	2005
YF-100	Booster	kero	SC	335	300	18.0	-	2015
YF-115	Upper	kero	SC	342	-	12.0	-	2015
YF-73	Upper	H2	GG	420	-	2.6	19	1987
YF-75	Upper	H2	GG	438	-	3.8	15	1994
YF-75D	Upper	H2	Expander	442	-	4.1	-	2016
YF-77	Booster	H2	GG	430	310	10.2	-	2016

All listed engines use liquid O_2 oxidizer. GG = gas generator, SC = staged combustion. Data from [1–3].

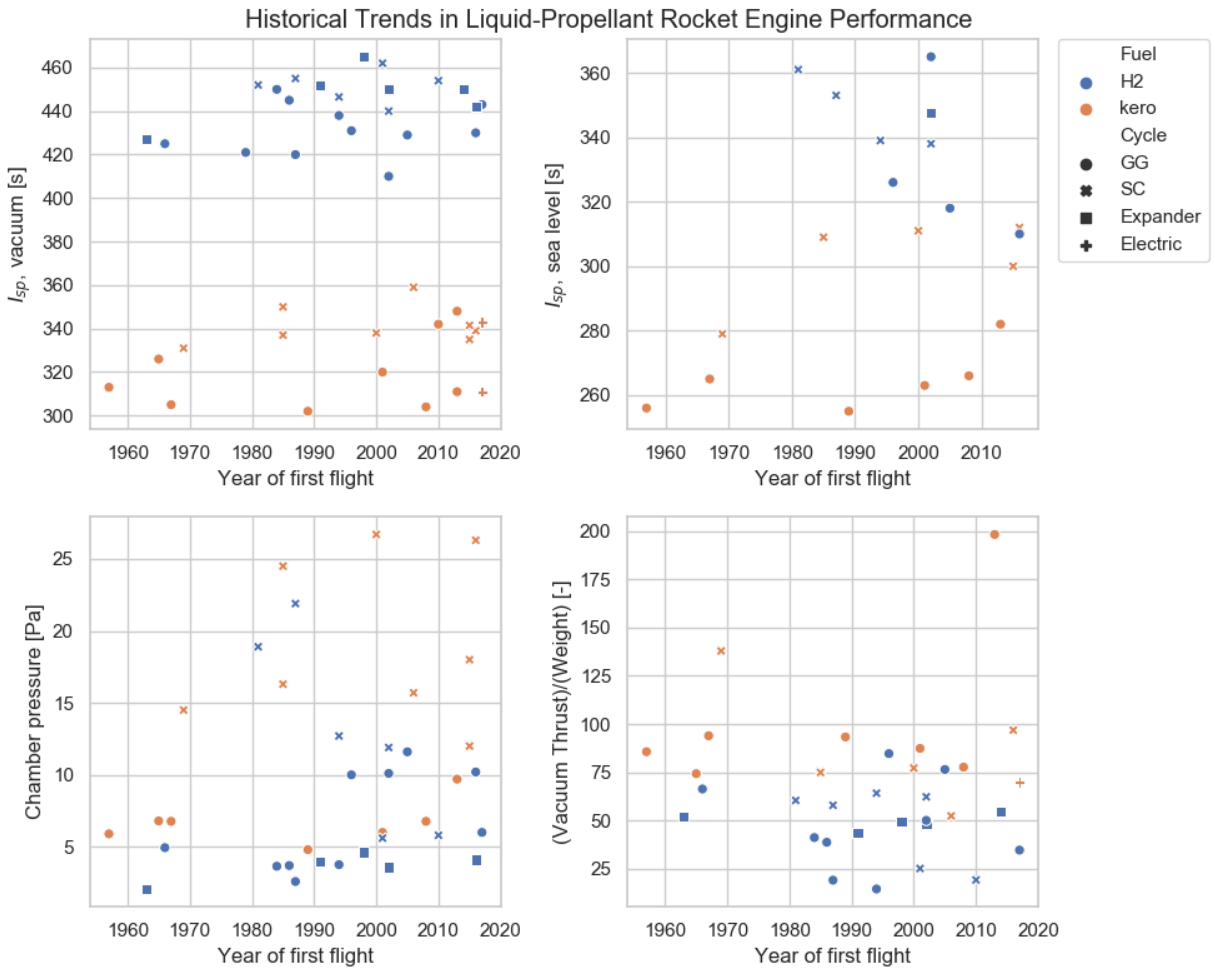

Fig. 1 Historical trends in engine performance. After 1975, there is no clear correlation of performance with time, thus these engines are likely representative of the performance of contemporary and near-future engines.

$$c_1 \approx g_0 \left(\frac{I_{sp,vac} + I_{sp,SL}}{2} \right)$$

This crude estimate results in surprisingly descent performance predictions [4].

Our performance model needs distributions on c_1 and c_2, which represent the possible variation in those parameters for a given technology choice. We arbitrarily choose to use triangular distributions, which are commonly used as a rough guess description when limited sample data is available. We will choose the parameters of the distributions based on the historical engine data. We fit a different distribution for each choice of propellant and engine cycle.

For upper stage engines, the distribution parameters are:

$$min = 0.98 g_0 \min_{e \in S}(I^e_{sp,vac})$$

$$max = g_0 \max_{e \in S}(I^e_{sp,vac})$$

$$mode = g_0 \operatorname{mean}_{e \in S}(I^e_{sp,vac})$$

where S is the set of historical engines matching the given propellant and cycle, and e is an engine from that set.

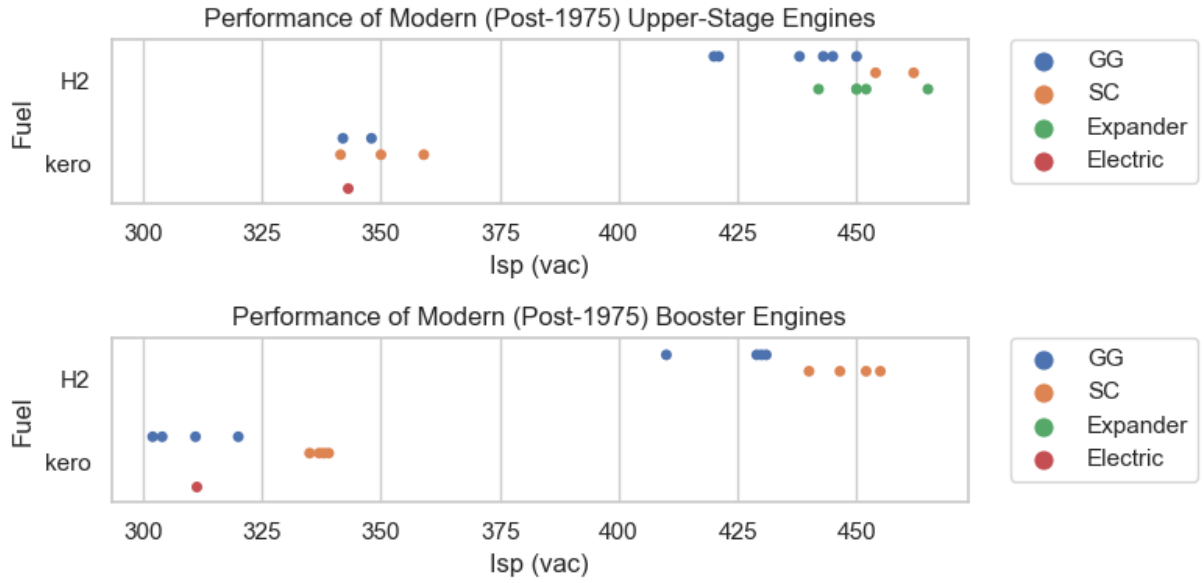

Fig. 2 Distribution of vacuum specific impulse of modern liquid propellant rocket engines, categorized by fuel and engine cycle. Unsurprisingly, hydrogen fuel and closed cycle (staged combustion or expander) engines have higher I_{sp}. The I_{sp} spread within each category is 6 s **to** 30 s

For booster engines, the mean of the vacuum and sea level I_{sp} is used, and the bounds of the distribution are spread by an additional 3% to account for the crudity of this estimate:

$$min = 0.95 g_0 \min_{e \in S} \left(\frac{I^e_{sp,vac} + I^e_{sp,SL}}{2} \right)$$

$$max = 1.03 g_0 \max_{e \in S} \left(\frac{I^e_{sp,vac} + I^e_{sp,SL}}{2} \right)$$

$$mode = g_0 \operatorname*{mean}_{e \in S} \left(\frac{I^e_{sp,vac} + I^e_{sp,SL}}{2} \right)$$

2. Inert mass fraction - expendable baseline

The inert mass fraction expendable baselines, E_1, E_2, represent the lower limit of achievable inert mass fraction for a particular technology choice. The values of E_1, E_2 are uncertain and hard to predict from first principles, as they result from a complicated engineering process. However, we can make an informed guess as to what is possible by examining historical trends in launch vehicle stages.

We compiled a sample of historical and active stages which have been sucessfully used in space launch vehicles; the data is drawn mainly from [5]. We segregate the data into boosters (first stages) and upper stages, as these have different structural design requirements. The present analysis only considers sequentially-staged launch vehciles, so we exclude boosters which cannot lift off under their own thrust.

First, we must determine whether there are historical trends in the inert mass fraction data. If there were a strong historical trend towards improving inert mass fraction, then a sample of historical stages would not be representative of the performance in modern and near-future stages. Examining Figure 3:

- For hydrogen upper stages there is no clear historical trend.
- For kerosene upper stages inert mass fraction has declined with time.
- For hygrogen boosters, there is only one example capable of liftoff under its own thrust (Delta IV Common Booster Core), so no historical trends can be observed.

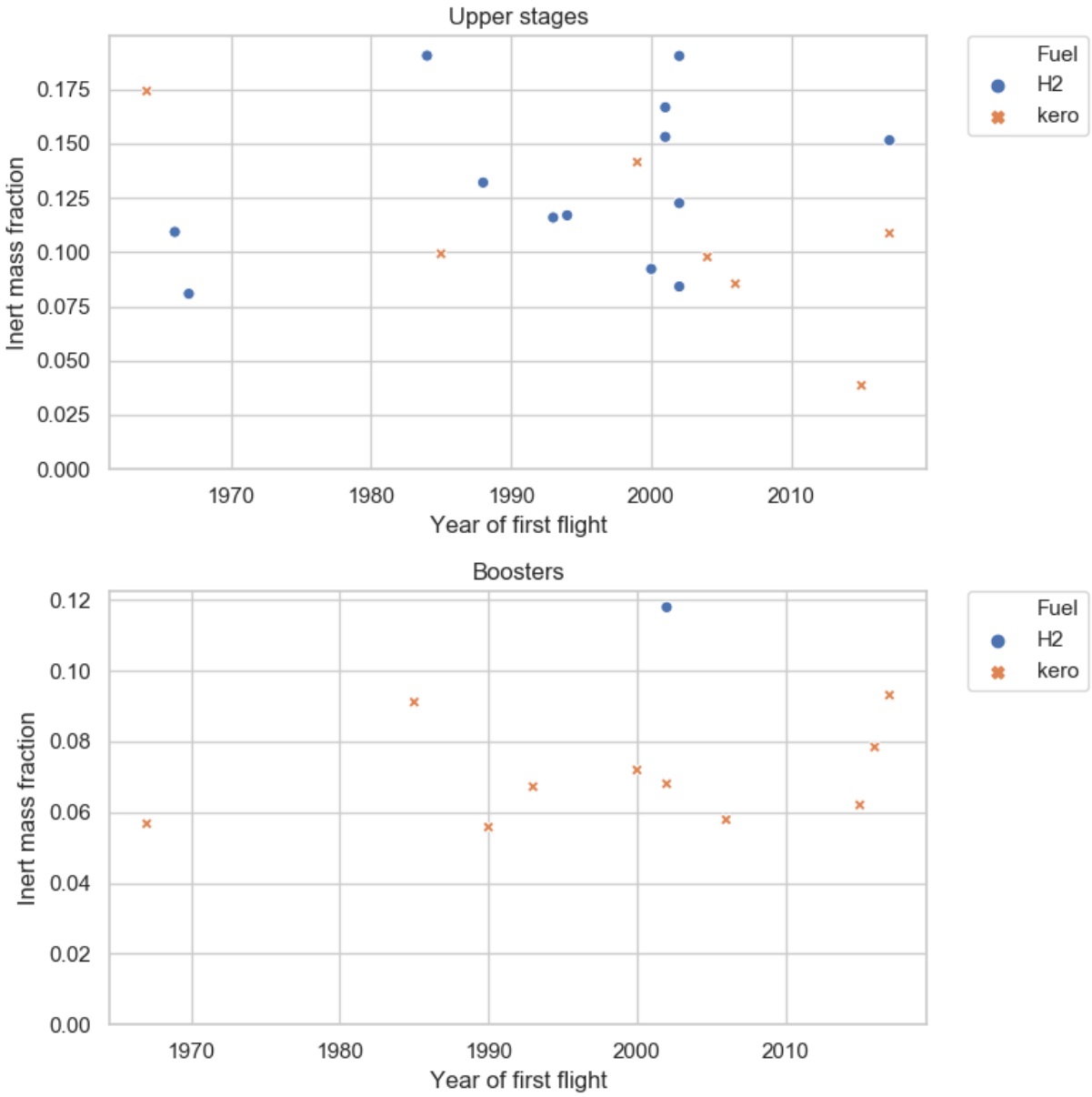

Fig. 3 Historical trends in stage inert mass. There are no clear trends with time, excepting the declining inert mass fraction of kerosene/O_2 upper stages.

- For kerosene boosters, there is no clear historical trend.

Next, we consider the relation between stage inert mass fraction and gross mass. There is reason to suspect that larger stages will have lower E, as some inert components (e.g. flight computer) have similar mass regarless of vehicle size. However, in Figure 4, we see that while there is a wider spread of inert mass fraction at low gross mass, the acheived *lower limit* of inert mass fraction does not show a clear sensitivity to gross mass.

The propellant technology choice has a noticeable effect on the inert mass fraction. H_2/O_2 stages tend to have higher inert mass fraction than kerosene/O_2 stages [Figure 5]. The lower denisty of hydrogen fuel requires larger tanks, increasing the ratio of tank mass to propellant mass.

Other technology choices (e.g. whether to have common or separate bulkheads between the fuel and oxidizer tanks) also effect the inert mass fraction. However, this study will not consider such detailed design choices.

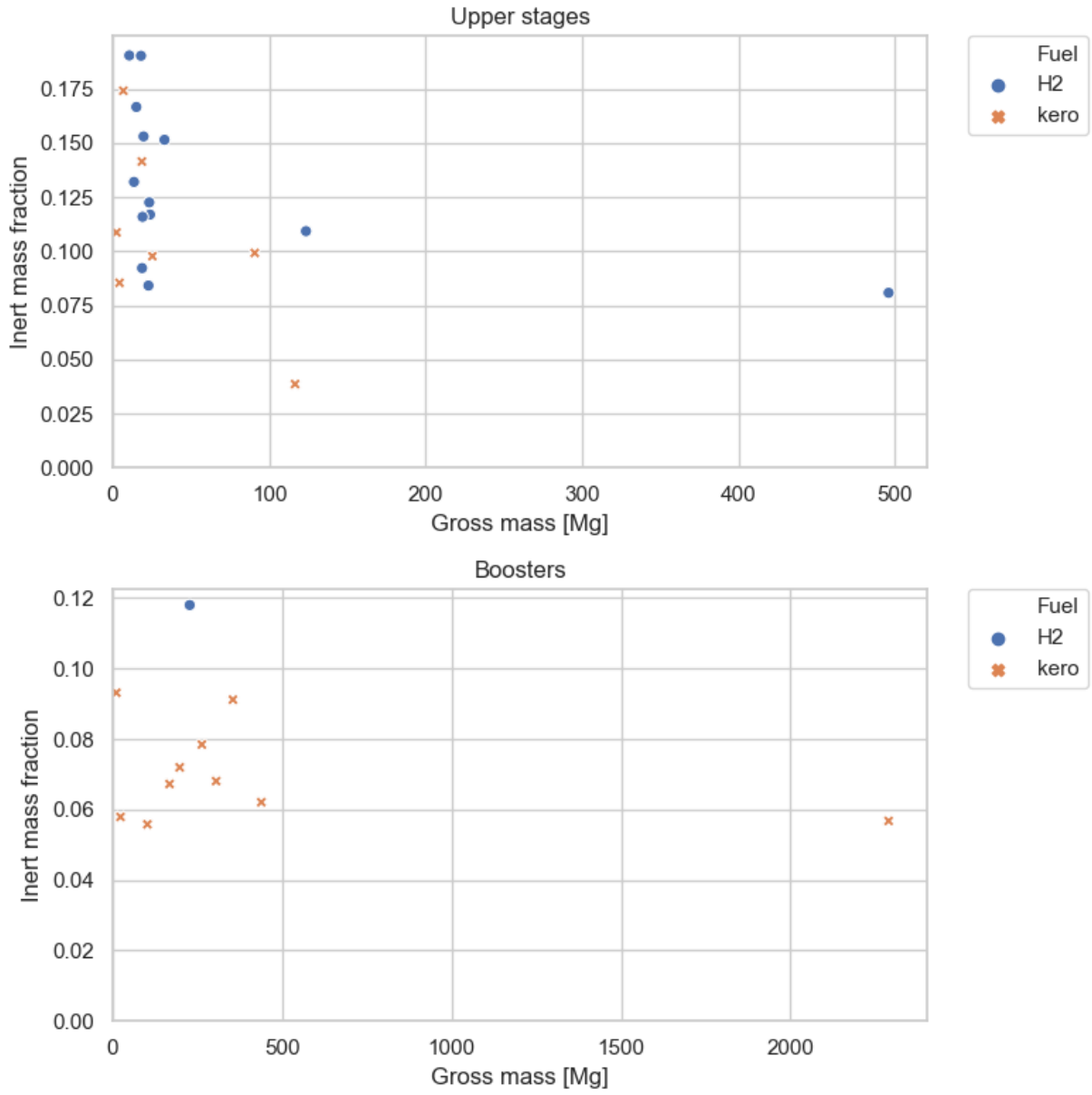

Fig. 4 Stage inert mass versus gross mass.

Table 2 Uncertianty distribution parameters on inert mass fraction lower limits.

Stage	Propellant choice	Triangular dist. params.		
		Min	Mode	Max
2, Upper	H_2 / O_2	0.080	0.085	0.090
	kerosene / O_2	0.040	0.050	0.060
1, Booster	H_2 / O_2	0.110	0.120	0.130
	kerosene / O_2	0.055	0.060	0.065

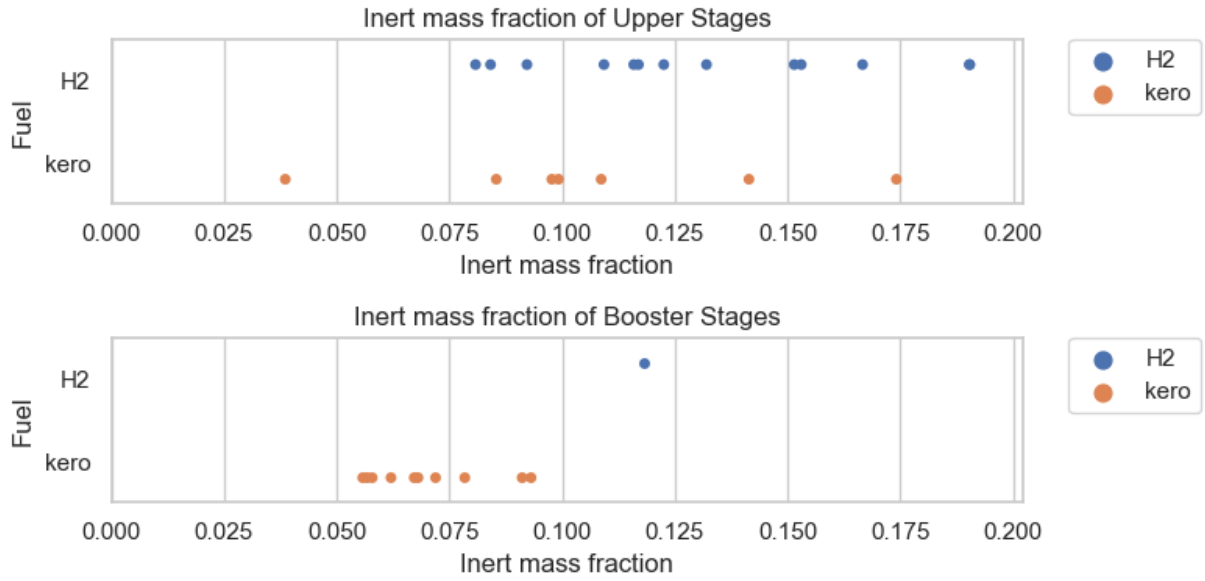

Fig. 5 Stage inert mass fraction by propellant choice.

B. Recovery Strategy Uncertainties

1. Winged / horizontal landing recovery

Need to estimate mass of recovery hardware H and recovery propellant P.

No winged recovery first stages have actually been operated, so we cannot infer these factors from a sample of historical systems. Instead, we estimate the mass of recovery hardware by three approximate soucres: high-fidelity studies of winged boosters undertaken by major aerospace institutions, a low fidelity study by Barry Hellman of Georgia Tech [6], and analogies to other winged vehicles.

First, we were able to find three high-fidelity winged booster concept designs: Khrunichev's Baikal booster [5], NASA/Boeing's Liquid Flyback Booster (dual configuration from [7]), and DRL's Liquid Flyback Booster [8]. These studies list the vehicle inert mass ($m_{inert,1} = m_{s,1} + m_{rh,1}$), the ascent propellant mass ($m_{p,1} - m_{pr,1}$) and the recovery propellant mass ($m_{pr,1}$). We compute H and P as:

$$H = \frac{m_{inert,1} - m_{p,1}\frac{E_1}{1-E_1}}{m_{inert,1}}$$

$$P = \ln\left(\frac{m_{pr,1}}{m_{inert,1}} + 1\right)$$

where E_1 is the base expendable inert mass fraction (assumed to be 0.06 for kero/O_2 and 0.12 for H_2/O_2), and $m_{p,1}\frac{E_1}{1-E_1}$ estimates the inert mass of an equivalent expendable stage.

Second, the Hellman study provides estimates of the inert and propellant masses for flyback and glideback boosters. These mass estimates are not based on detailed design considerations, but rather on subsystem mass-estimation relationships developed at Georgia Tech [9].

Our third source is analogy to other winged vehicles. We considered the subsystems which would need to be added to an expendable booster to enable winged recovery (wing, stabiliser, landing gear, surface controls, hydraulics, thermal protection, air breathing propulsion) and computed the fraction of the empty mass is made up by these systems as an estimate of H. We considered winged vehicles which cover a variety of missions, sizes and construction technology (STS orbiter, Lockheed C-141, Gulfstream G550, Boeing 787-8).

The resulting estimates of H are shown in Figure 6. For powered-flight winged boosters, there is good agreement between the three estimate types. We can have some confidence that H for powered-flight winged boosters is in the range 0.49 to 0.65, i.e. a powered-flight winged booster will have $1/(1-H) = 2.0$ to 2.8 times the dry mass of an expendable

booster with the same propellant load. Glider winged boosters can be expected to be somewhat lighter, with H in the range of 0.38 to 0.54, i.e. having 1.6 to 1.8 times the dry mass of an expendable booster with the same propellant load. We represent the uncertainty on H with a triangular distribution, the parameters of which are given in Table 3.

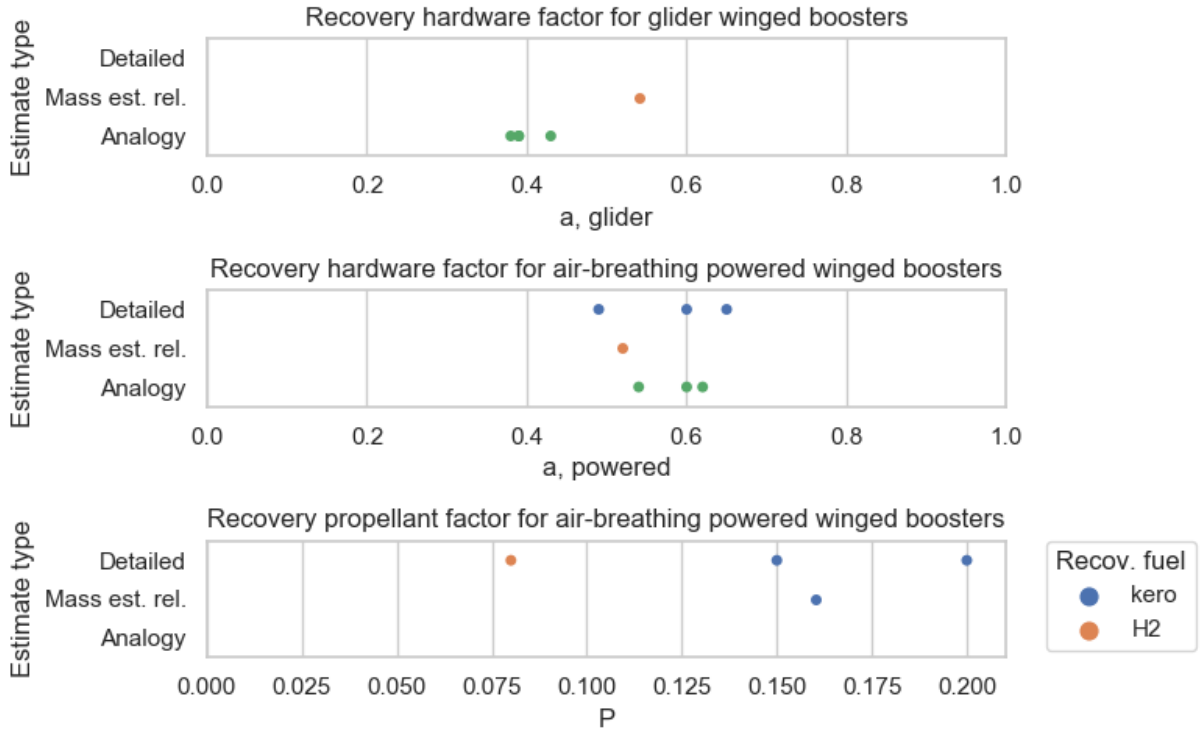

Fig. 6 Various estimates of the recovery hardware factor H for glider and powered horizontal-landing boosters. Data from [5–8]

Table 3 Uncertainty distribution parameters of the recovery hardware factor H for glider and powered horizontal-landing boosters.

	Triangular dist. params.		
	Min	Mode	Max
Glider	0.380	0.426	0.540
Powered	0.490	0.574	0.650

2. Propulsive landing

Need to estimate recovery hardware mass factor H.

Propulsive landing boosters require extra hardware not needed on an expendable booster. On most flown or proposed designs, this extra hardware includes aerodynamic control surfaces and actuators, landing gear*, and thermal protection [3, 10–12].

Although three propulsive landing boosters have been flown, we could not find reliable, publicly available data on the masses of the extra hardware systems. Instead, we will crudely estimate the mass of these systems by analogy to other aerospace vehicles (STS orbiter, Lockheed C-141, Gulfstream G550, Boeing 787-8). On these vehicles, the

*It may be possible to forgo landing gear by high-precision landing on a support structure [10], however this difficult technique has yet to be demonstrated.

surface controls and actuators make up 2 to 5% of the vehicle empty mass, and landing gear 7 to 8%. Although the design of aircraft landing gear is quite different, this is a decent first guess. We guess that thermal protection adds another 2% to 4% (TODO although there is a trade-off against entry burn Δv). Thus, we expect H to be 0.11 to 0.17, i.e. a propulsive landing booster should have 1.1 to 1.2 times the dry mass of an expendable booster with the same propellant load. Because these estimates are crude, we expand the bounds by 0.02 on either side when choosing the parameters of the triangular distribution (Table 4).

Table 4 Uncertainty distribution parameters of the recovery hardware factor H for propulsive-landing boosters.

	Triangular dist. params.		
	Min	Mode	Max
Propulsive landing	0.09	0.14	0.19

3. Parachute recovery

Need to estimate recovery hardware mass factor H.

The Space Shuttle Solid Rocket Boosters (SRBs) and the Ariane 5 EAP boosters are the only operational examples of parachute recovery of full space launch vehicle stages. The mass of the SRB parachutes were 3.5% of booster dry mass [13], and entry thermal protection added another few percent. Thus, we expect a to be in the range 0.05 to 0.08.

owever, the SRB example is not indicative of parachute recovery for liquid boosters. Solid rocket boosters must contain a much higher internal pressure than pump-fed liquid stages, and are therefore have a stronger structure which is more robust to entry loads. Attempts to fully recover liquid stages via parachute have failed, with the stages breaking up during reentry [14].

Partial recovery via parachute may be more feasible for liquid boosters, as a compact engine pod could more easily survive entry loads. United Launch Alliance has proposed to recover the engines of Atlas V (or the next-generation Vulcan) via parachutes and mid-air capture [15, 16]. This proposal also includes an inflatable heat shield (Hypersonic Inflatable Aerodynamic Decelerator, HIAD) which will protect and decelerate the recovery vehicle. The proposed 10 m HIAD is estimated to have a mass of 1.5 Mg [17], about 13% of the recovery vehicle mass. Including parachutes as well, the H value for this strategy should be ≈ 0.17. Recovery via mid-air capture should reduce recovery operations and refurbishment costs compared to recovery in the ocean.

Table 5 Uncertainty distribution parameters of the recovery hardware factor H for parachute recovery boosters.

	Triangular dist. params.		
	Min	Mode	Max
Parachutes	0.050	0.065	0.080
Parachutes and inflatable heat shield	0.150	0.170	0.190

II. Cost-Related Uncertainties

The uncertainties in the cost model were quantified by assessing the variability in the cost data provided in TRANSCOST 8.2 [18]. For each cost-estimating relationship, we regressed the cost vs. mass data provided in [18]. From this regression we not only re-obtained the central values of the model parameters a and x, but also obtained confidence intervals on these parameters. In our Monte Carlo analysis, we drew the a and x parameters from triangular distributions with:

- Minimum set to the lower bound of the parameter's 95% confidence interval.
- Mode set to the estimated value of the parameter.
- Maximum set to the upper bound of the parameter's 95% confidence interval.

We also assigned dispersions to TRANSCOST's cost multiplier factors (f's) based on the value ranges suggested in TRANSCOST.

References

[1] Sutton, G. P., *History of Liquid Propellant Rocket Engines*, AIAA, Reston, Viginia, 2006.

[2] Wikipedia contributors, "Comparison of orbital rocket engines — Wikipedia, The Free Encyclopedia," , 2018. URL https://en.wikipedia.org/wiki/Comparison_of_orbital_rocket_engines, accessed: 2018-07-25.

[3] Space Exploration Technologies, "Falcon 9," http://www.spacex.com/falcon9, 2018.

[4] Alber, I. E., *Aerospace Engineering on the Back of an Envelop*, Springer-Verlag Berlin Heidelberg, Berlin, Germany, 2012.

[5] Isakowitz, S. J., Hopkins, J. B., and Hopkins, J. P., Jr., *International Reference Guide to Space Launch Systems*, American Institute of Aeronautics and Astronautics, Reston, Viginia, 2004.

[6] Hellman, B. M., "Comparison of Return to Launch Site Options for a Reusable Booster Stage," Tech. rep., Georgia Institute of Technology, 08 2005.

[7] Healy, T. J., "Shuttle Liquid Fly Back Booster Configuration Options," *JANNAF Propulsion Meeting*, 1998.

[8] Sippel, M., International Astronautical Congress (IAF), American Institute of Aeronautics and Astronautics, 2003, Chaps. Long-Term / Strategic Scenario for Reusable Booster Stages. doi:10.2514/6.IAC-03-V.4.02, URL https://doi.org/10.2514/6.IAC-03-V.4.02, 0.

[9] Rohrschneider, R. R., "Development of a Mass Estimating Relationship Database for Launch Vehicle Conceptual Design," , 2002. URL http://www.ssdl.gatech.edu/sites/default/files/papers/mastersProjects/RohrschneiderR-8900.pdf.

[10] Musk, E., "Making Humans a Multi-Planetary Species," *New Space*, Vol. 5, No. 2, 2017, pp. 46–61. URL https://doi.org/10.1089/space.2017.29009.emu.

[11] Blue Origin, "New Glenn," https://www.blueorigin.com/new-glenn, 2018. Accessed: 2018-02-18.

[12] Ballistic Missile Defense Organization, "Delta Clipper-Experimental Fact Sheet," https://www.hq.nasa.gov/pao/History/x-33/dcx-facts.htm, ????

[13] Wolf, D., and Runkle, R., "Space Shuttle Solid Rocket Booster Lightweight Recovery System," Tech. rep., 1996.

[14] Spencer, H., "Falcon Rockets to Land on Their Toes," *New Scientist*, 2011. URL https://www.newscientist.com/blogs/shortsharpscience/2011/09/falcon-rockets-to-land-on-thei.html.

[15] Gravlee, M., Kutter, B., Zegler, F., Mosley, B., and Haggard, R., "Partial Rocket Reuse Using Mid-Air Recovery," *AIAA SPACE 2008 Conference and Exposition*, AIAA, 2008.

[16] Ragab, M., and Cheatwood, F. M., AIAA SPACE Forum, American Institute of Aeronautics and Astronautics, 2015, Chap. Launch Vehicle Recovery and Reuse. doi:10.2514/6.2015-4490, URL https://doi.org/10.2514/6.2015-4490, 0.

[17] Bose, D., Shidner, J., Winski, R., Zumwalt, C., and Cheatwood, F., "The Hypersonic Inflatable Aerodynamic Decelerator (HIAD) Mission Applications Study," *9th International Planetary Probe Workshop*, 2012.

[18] Koelle, D. E., *Handbook of Cost Engineering for Space Transportation Systems with TRANSCOST 8.2*, Trans Cost Systems, Ottobrunn, Germany, 2013.